Highly Directive Degenerate Band Edge Crystal-Type Resonator Antenna

***Salih Yarga**, Kubilay Sertel, John L. Volakis*

ElectroScience Lab., Electrical and Computer Engineering Dept., The Ohio State University,
1320 Kinnear Rd., Columbus, OH 43212, USA,
e-mail: yarga.1@osu.edu, sertel.1@osu.edu, volakis.1@osu.edu

1. Introduction

In recent years, there is a growing interest in compact high-gain antennas with a single feed for civil/tactical wireless communication systems. Electromagnetic band gap (EBG) materials with embedded antennas/feeds offer new design possibilities [1-2]. Although defect based EBG antennas achieve high directivities, they require comparatively large physical sizes for practical applications. As an alternative, Fabry-Perot transmission resonances of EBGs can be utilized. EBGs are primarily composed of isotropic materials, but their scope has extended to a variety of materials, including metallic structures, anisotropic dielectrics [3-4] as well as non-reciprocal materials. Among these, degenerate band edge (DBE) crystals employ materials displaying in-plane uniaxial anisotropy to yield a maximally flat k-ω diagram. Fig. 1a depicts a typical unit cell configuration with two adjacent uniaxial layers misaligned with respect to each other, followed by an isotropic layer. The corresponding band diagram for the listed material parameters is shown in Fig. 1b. As seen, the periodic arrangement of this unit cell displays a higher mode density located at the band edge as compared to conventional 1-D EBGs. This increased density of modes implies a stronger resonance manifesting itself into sharper transmission peaks (i.e. Fabry-Perot resonances of higher quality factors) for structures of finite thickness [3-4]. Thus, DBE crystals can reduce the form factors of conventional EBG structures since they require fewer unit cells to realize the modes.

The theory of DBE crystals and their use in improving radiation of small sources (embedded within these crystals) has been presented before [3-4]. Specifically, a design that employs metallic strips to mimic the required anisotropy was realized and shown to support DBE modes [4]. However, the demonstration in [4] achieved only 38% aperture efficiency. This was due to metallic inclusions that have much higher loss and weak level of anisotropy resulting in larger structures. In this paper, we present a new realization of the DBE crystal that efficiently utilizes the physical aperture. Specifically, the anisotropy is realized by combining two isotropic materials (i.e. commercially available Barium Titanate ($BaTiO_3$) and Alumina (Al_2O_3)) in an alternating manner. These uniaxial layers are then stacked to form the DBE crystal. However, designing structures having relatively small apertures requires concurrent presence of DBE resonances and dielectric resonator antenna (DRA) type lateral modes (see Fig. 2).

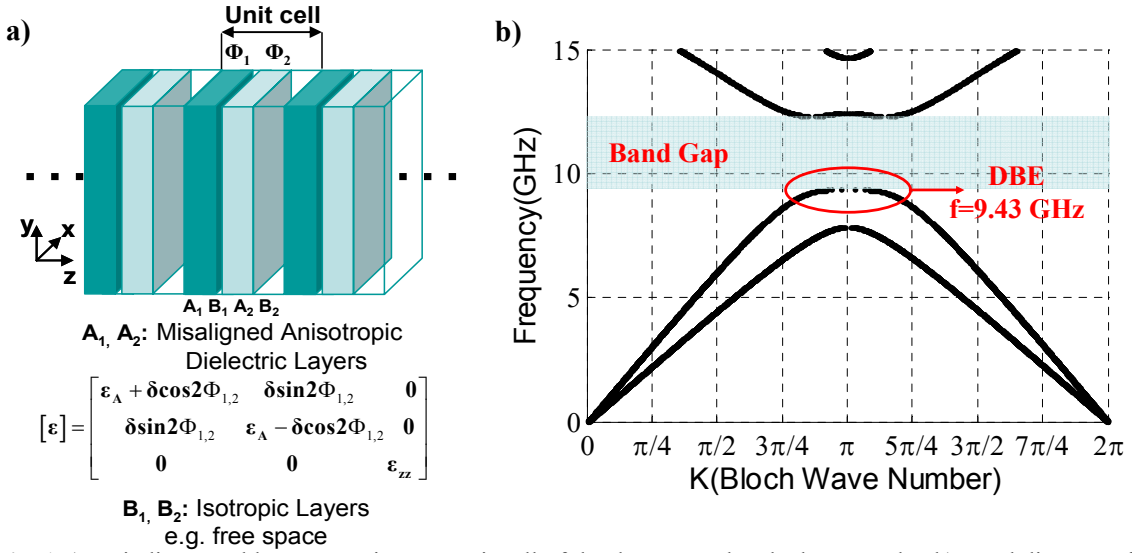

Fig. 1 a) Periodic assembly representing one unit cell of the degenerate band edge crystals. b) Band diagram of the periodic structure shown in a) for layer thicknesses of $\mathbf{h_{A1}}$= $\mathbf{h_{A2}}$= $\mathbf{h_{B2}}$=1 mm, $\mathbf{h_{B1}}$=0.25 mm, and tensor parameters $\boldsymbol{\varepsilon_A}$=31.39, $\boldsymbol{\delta}$=13.61, $\boldsymbol{\Phi=\Phi_1-\Phi_2=\pi/4}$.

2. Concept and Design

The proposed DBE antenna, shown in Fig. 2, consists of three identical structures (each having two misaligned uniaxial layers followed by air gaps as seen in Fig. 2a and 2b) situated over a sufficiently large, finite ground plane. A microstrip fed slot on the ground plane is employed to feed the DBE crystal from the bottom (Fig. 2c), and serves to minimize possible disturbance of the DBE mode. As seen, the antenna geometry allows for several parameter variations to achieve optimum performance. These parameters can be classified as follows: 1) DBE modal parameters (layer thickness and seperations, h_{xx}, as well as misalignment angles, Φ_1 and Φ_2) that can be tuned to yield the DBE response for $\hat{\mathbf{z}}$ -propagating waves 2) Lateral modal parameters (layer lengths, ℓ_{xx}, and widths, w_{xx}, along with ground plane dimensions, ℓ_g, see Fig. 2b), 3) Impedance matching/coupling parameters (length and width of the slot and stub, ℓ_s, w_s, ℓ_{stub}, and w_m, shown in Fig. 2c). First, we proceed with the design of the DBE modal parameters.

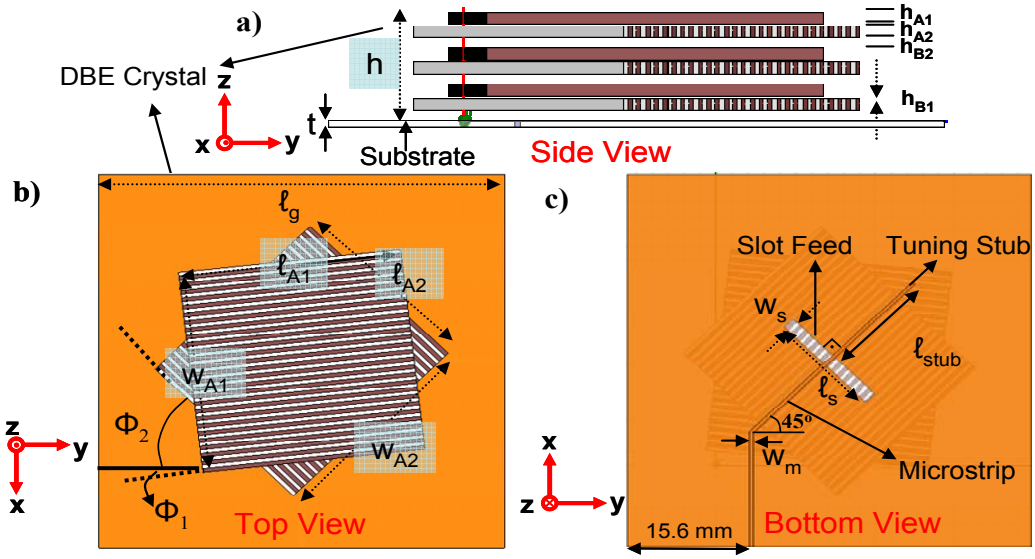

Fig. 2. Sketch of the proposed DBE antenna. a) Side view of the layers showing the periodicity supporting the DBE modes along the $\hat{z}$ direction (vertical) b) Top view depicting the lateral dimensions c) Bottom view showing the feeding slot and the coupled microstrip dimensions.

2.1 DBE Modes Design for $\hat{z}$ -directed Plane Wave Excitation

The simplest building block of a DBE crystal is a unit cell consisting of two uniaxial dielectric layers (A_1 and A_2 in Fig. 1), misaligned with respect to each other by an angle ($\Phi = \Phi_1 - \Phi_2$). These two layers are then followed by an isotropic layer (B_2 layer in Fig. 1). A small gap (B_1) between the A_1 and A_2 layers can be introduced to model manufacturing inaccuracies and this also allows for greater design flexibility. Proper tuning of the layer thicknesses in the unit cell yields a maximally flat k-ω band edge behavior referred to as the degenerate band edge (DBE). Since readily available low-loss anisotropic dielectric materials (such as single-crystal rutile, TiO_2) are costly, we proceeded to realize the anisotropy artificially. In this context, employing metallic inclusions [4] and stacked dielectrics of different permittivities have been found effective in achieving large uniaxial anisotropy. Unfortunately, the former suffers from severe conduction losses. Therefore, we only employ purely dielectric layers to realize anisotropy. Specifically, we chose $BaTiO_3$ ($\varepsilon_r \approx 80$, $\tan\delta = 3.7\times10^{-4}$ at 2.13 GHz) and Al_2O_3 ($\varepsilon_r \approx 10$, $\tan\delta = 2.8\times10^{-4}$ at 3.37 GHz) to form the uniaxial crystal layers. This choice allows for high contrast dielectric constants known to translate to higher anisotropy in the assembled structure. Consequently, when the individual laminate thicknesses are much smaller than the wavelength, the alternating stacks of these laminates exhibits the equivalent tensor given by: $\varepsilon_{xx} = \varepsilon_{zz} = 45$, $\varepsilon_{yy} = 17.78$. First, we proceed with the design of the DBE dispersion diagram using 1 mm thick layers of the uniaxial two-tone dielectrics ($BaTiO_3$ and Al_2O_3). Fig. 1b shows the band diagram of the unit cell shown in Fig. 1a. The DBE response is achieved when the air layer thicknesses are $h_{B1} = 0.25$ mm (10 mils) and $h_{B2} = 1$ mm with the misalignment angle $\Phi = 45°$. As seen, the geometry exhibits a DBE mode at 9.43 GHz and a double band edge for the upper edge of the stop band. Obviously, this band diagram exhibits the modes of a layered medium composed of DBE unit cells having infinite

lateral dimensions. Practically, such modes must be realized using a finite DBE crystal (in the lateral and vertical directions). However, before proceeding with the characterization of the 3-D finite DBE crystal, the layer thicknesses are determined using a one dimensional (1-D) analysis. One dimensional periodic structures of finite thickness demonstrate Fabry-Perot (FP) transmission resonance frequencies at which the fields exhibit standing wave patterns (typically of high amplitudes within the structure). Although crystal tranmissivity vanishes at the exact band edge frequencies (e.g. 9.43 GHz in Fig. 2), the diminishing group velocity can still be harnessed in the vicinity of the band edge, namely at the frequency of the closest FP transmission peak. Hence, we proceed with the 3-unit cell structure that is as thin as $0.28\lambda_o$ at 8.91 GHz, the closest FP peak for the DBE crystal over the ground plane shown in Fig. 2.

2.2 DBE Antenna Design

We choose to feed the DBE resonator with a slot as shown in Fig. 2. As usual, the slot is then excited from below using a microstrip line, thus, avoiding possible disturbance of the DBE mode. We do remark, however, that the DBE mode is generally associated with elliptical polarization. Hence, the excitation should be designed to ensure optimal coupling to the DBE mode (once the DRA resonance is achieved). The feeding slot was oriented perpendicular to the rectangular rods at the bottom-most layer to match the polarization of the magnetic field for reception under plane wave illumination at the FP resonance. The simulations were carried out using a (3-D) finite element method (FEM)-based commercial software (Ansoft HFSS Version 10.1.1). In the model, the rectangular rods of $BaTiO_3$ and Al_2O_3 (both having tan δ=1.9×10−3 obtained from loss characterization) were identically modeled rather than using the equivalent tensor to avoid possible homogenization inaccuracies. Also, layer lengths are set to ℓ_{A1}=28 mm and ℓ_{A2}=24.5 mm, layer widths are set to w_{A1}= w_{A2}=27.43 mm and the microstrip width (w_m) was 0.65 mm. Further, the feeding slot was ℓ_s=17 mm long and w_s=1.6 mm wide. For the microstrip feed below the slot, the substrate was an Al_2O_3 laminate of thickness 0.5 mm (20 mil) with ℓ_g=50.8 mm. We remark that mode confinement within the finite crystal, resonance location and matching are governed by the overall assembly. So, the misalignment angle was fine tuned to Φ= 2π/7 (Φ_1= π /28 and Φ_2= π /4 in Fig. 2) for optimal bandwidth. The FP peak then shifted to 8.71 GHz. Fig. 4b depicts the return loss of the DBE antenna exhibiting structural modes. Moreover, a -10 dB return loss bandwidth of 337.1 MHz (3.85%) is achieved covering the entire bandwidth of the DBE FP resonance.

The corresponding directivity is plotted in Fig. 3. As seen, the 3dB directivity bandwidth is around 347.1 MHz (3.97%) and recovers the FP peak. More importantly, a maximum directivity of 10.17 dB is achieved at 8.785 GHz with an aperture efficiency of ηap=125.56%, referenced to the top surface of the crystal. We should note that an aperture efficiency greater than 100% is not unorthodox if the side walls of the DBE crystal are considered. For our case, the side walls contribute to the main beam as well, increasing the directivity. We should also note that, the finite ground plane is sufficiently large to emulate an infinite ground plane. More importantly, since the dielectric losses were kept remarkably low, the realized gain (including mismatch) is only 1 dB to 1.5 dB below the directivity level, implying 70-80% radiation efficiency. Having completed a satisfactory design, we now proceed with an experimental verification of the DBE-DRA antenna performance.

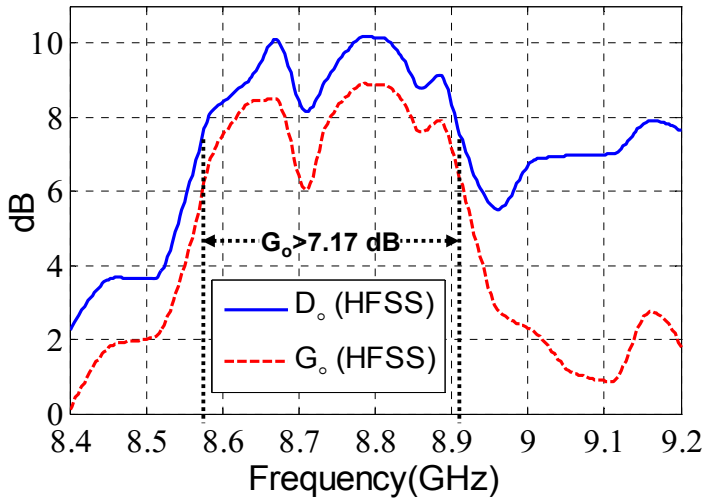

Fig. 3. The directivity and realized gain of the DBE antenna for **Φ**=2π/7.

3. Experimental Verification

The manufactured antenna assembly is shown in Fig. 4a. As seen, the 3-layer DBE crystal is placed over the finite ground plane and the microstrip feed is excited through an SMA connector. Fig. 4b gives the measured return loss as compared to simulations. Given the many steps used to fabricate the prototype in Fig. 4a, the observed agreement between measurements and simulations is truly remarkable (particularly the S_{11} level at around 8.64 GHz). Although the

measured bandwidth is slightly smaller than predicted, it can be enlarged by tuning the feeding aperture (slot, stub and microstrip). The far-field pattern of the realized antenna measured in an anechoic chamber (Results are not included here). Again, a reasonable agreement is observed between measured and computed patterns. More specifically, a gain of 7.42 dB was measured, and this is only 1 dB below the computed value.

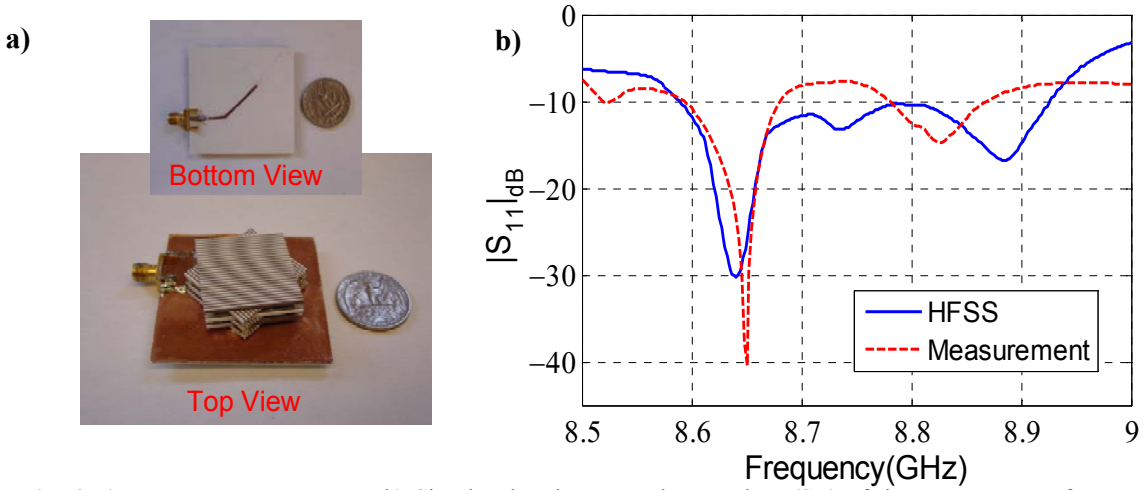

Fig. 4. a) DBE antenna prototype. b) Simulated and measured return loss (S_{11}) of the DBE antenna for **Φ**= $2\pi/7$.

4. Acknowledgments

This work was supported by the U.S. Air Force Office of Scientific Research under the grant FA9550-04-1-0359. Also, the authors wish to thank L. Zhang and Prof. H. Verweij for fabricating the ceramic laminates.

5. Conclusion

We demonstrated that the DBE crystals offer unique characteristics for antenna applications. The anisotropic nature of such crystals allowed for greater design flexibility to realize new resonant modes that can be harnessed to develop smaller directive antennas. For the first time, the DBE crystal and its associated anisotropy was realized using a set of alternating Al_2O_3 and $BaTiO_3$ rods. Finite size layers of these alternating rods were then designed and arranged to form a periodic assembly as small as $0.79\lambda_o$ x $0.80\lambda_o$ in aperture and $0.28\lambda_o$ thick. Due to the finite size of the crystal, the developed antenna is comparable to a dielectric resonator antenna operating at the DBE modes (we therefore called it a DBE-DRA antenna). To the best of our knowledge, this is one of smallest metamaterial antenna designs for directive radiation. The DBE antenna had a peak directivity of 10.16 dB, a -10 dB return loss bandwidth of 3.85% and a 3 dB directivity bandwidth of 3.97%. A maximum aperture efficiency of 126.55% (based on the top surface of the crystal) was achieved. This aperture efficiency should be compared to typical aperture efficiencies of 30% to 90% (optimum gain horns have $\eta ap \approx 50\%$), and 50% to 80% for circular reflectors.

6. References

1. E. R. Brown, C. D. Parker, and E. Yablonovitch, “Radiation properties of a planar antenna on a photonic-crystal substrate,” Journal of the Optical Society of America B., vol. 10, no. 2, Feb. 1993, pp. 404-407.

2. N. Gu´erin, S. Enoch, G. Tayeb, P. Sabouroux, P. Vincent, and H. Legay, “A metallic fabryperot directive antenna,” IEEE Trans. Antennas Propagat., vol. 54, no. 1, Jan. 2006, pp. 220–224.

3. A. Figotin and I. Vitebskiy, “Gigantic transmission bandedge resonance in periodic stacks of anisotropic layers,” Physical Review E, vol. 72, no. 3, Sept. 2005, pp. 036 619–036 630.

4. S. Yarga, K. Sertel, and J. L. Volakis, “Degenerate band edge crystals for directive antennas,” IEEE Trans. Antennas Propagat., vol. 56, no. 1, Jan. 2008, pp. 119-126.